Electrocatalysis

Deutsche Ausgabe: DOI: 10.1002/ange.201511804
Internationale Ausgabe: DOI: 10.1002/anie.201511804

Full Kinetics from First Principles of the Chlorine Evolution Reaction over a $RuO_2(110)$ Model Electrode

*Kai S. Exner, Josef Anton, Timo Jacob, and Herbert Over**

Abstract: *Current progress in modern electrocatalysis research is spurred by theory, frequently based on ab initio thermodynamics, where the stable reaction intermediates at the electrode surface are identified, while the actual energy barriers are ignored. This approach is popular in that a simple tool is available for searching for promising electrode materials. However, thermodynamics alone may be misleading to assess the catalytic activity of an electrochemical reaction as we exemplify with the chlorine evolution reaction (CER) over a $RuO_2(110)$ model electrode. The full procedure is introduced, starting from the stable reaction intermediates, computing the energy barriers, and finally performing microkinetic simulations, all performed under the influence of the solvent and the electrode potential. Full kinetics from first-principles allows the rate-determining step in the CER to be identified and the experimentally observed change in the Tafel slope to be explained.*

The chlorine evolution reaction (CER) constitutes the anodic reaction of the chlor-alkali and the HCl electrolysis. Both are important large-scale industrial processes, which annually produce 95% of the 70 million tons of chlorine worldwide.[1] Two chloride anions need to be successively discharged at the dimensionally stable anodes with the catalytically active component RuO_2,[2] thereby forming gaseous chlorine in the so-called chlorine evolution reaction CER: $2\,Cl^- \rightarrow Cl_2 + 2\,e^-$.[3]

A single-crystalline $RuO_2(110)$ electrode may be envisioned as an appropriate model system for studying the elementary processes in the CER.[4] Extensive experimental studies of the CER over a single-crystalline $RuO_2(110)$ electrode go back to the 1980s.[5] Consonni et al. determined a Tafel slope of 40 mV dec^{-1} for small overpotentials and a reaction order of +1 with respect to chloride ions, whereas no pH effect was observed. Guerrini et al. reexamined this model system in 2005 and confirmed a Tafel slope of 40 mV dec^{-1} for small overpotentials in the first Tafel region.[6] However, for higher overpotentials, they found a significantly increased Tafel slope of about 80 mV dec^{-1}, without providing further explanation for this observation.

To gain molecular insight into the CER over $RuO_2(110)$, the stable surface terminations of the $RuO_2(110)$ model catalyst for given pH and the overpotential η were identified based on ab initio thermodynamics.[7–14] The overpotential η is defined as the excess electrode potential with respect to the standard half-cell potential of CER (1.36 V). In ab initio thermodynamics, the Gibbs free energies ΔG are calculated by density functional theory (DFT) for a variety of possible surface configurations under reaction conditions. Only those surface terminations are considered stable that minimize ΔG for given values of pH and the overpotential η[7,15,16] (Figure 1).

Herein, the solvent effect was estimated by separate electronic calculations with two explicit water molecules per adsorbate in the (2×1) unit cell. In previous studies this approach has already been proven to be applicable.[17] Further details about the DFT calculations (Supporting Information, Section 1) and the construction of surface phase diagrams are given in the Supporting Information, Section 2.

Under typical CER reaction conditions ($\eta > 0$ V, pH = 0), all undercoordinated ruthenium sites Ru_{cus} of the $RuO_2(110)$

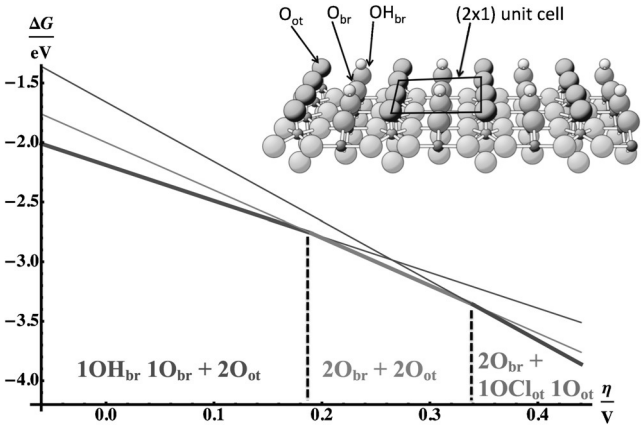

Figure 1. Stable surface terminations of the model catalyst $RuO_2(110)$ in equilibrium with H^+, Cl^-, and H_2O at $T = 298.15$ K, $a(Cl^-) = 1$, and pH = 0 as a function of the overpotential η. The nomenclature of the surface structures is referred to a (2×1) unit cell, indicating all surface species in the unit cell without the attached metal atom. ($2\,O_{br} + 2\,O_{ot}$) contains two O_{br} bridging two Ru_{2f} sites and two on-top oxygen atoms O_{ot} attached to Ru_{cus} sites (stick and ball model; oxygen atoms: large black balls). The ($1O_{br}1OH_{br} + 2O_{ot}$) surface, which is denoted as fully oxygen-covered $RuO_2(110)$ surface, constitutes the thermodynamically most stable phase for $\eta < 0.19$ V and therefore is considered to be the active surface under CER reaction conditions. The adsorption of chlorine on the catalyst's surface takes solely place on the O_{ot} atoms forming an OCl_{ot} precursor structure for CER.

[*] Dr. K. S. Exner, Prof. Dr. H. Over
Physikalisch-Chemisches Institut, Justus-Liebig-Universität
Heinrich-Buff-Ring 17, 35392 Gießen (Germany)
E-mail: herbert.over@phys.chemie.uni-giessen.de
Dr. J. Anton, Prof. Dr. T. Jacob
Institut für Elektrochemie, Universität Ulm
Albert-Einstein-Allee 47, 89069 Ulm (Germany)
and
Helmholtz-Institut-Ulm (HIU)
Helmholtzstrasse 11, 89081 Ulm (Germany)

Supporting information for this article can be found under: http://dx.doi.org/10.1002/anie.201511804.

surface are capped by on-top oxygen O_{ot} (Figure 1), while the bridging oxygen O_{br} are partially saturated by hydrogen depending on the overpotential η. The $(1\,O_{br}1\,OH_{br}+2\,O_{ot})$ surface, which is denoted as fully oxygen-covered $RuO_2(110)$ surface, constitutes the thermodynamically most stable phase for $\eta<0.19$ V and therefore is considered to be the active surface under CER reaction conditions. The adsorption of chlorine on the catalyst's surface takes solely place on the O_{ot} atoms forming an OCl_{ot} precursor structure for CER. It turns out that the adsorption of chlorine on the O_{ot} surface atoms is by 0.7 eV energetically more favored than on O_{br}.[15] The corresponding OCl_{ot} adsorbate structure, which becomes thermodynamically stable for $\eta>0.34$ V, is therefore identified with the precursor state for CER over $RuO_2(110)$, consistent with an early proposal of Burke and O'Neill in 1979.[18] In the overpotential range up to about 0.2 V, the actual CER over $RuO_2(110)$ proceeds on two different active sites (cf. Figure 1): O_{ot} next to O_{br} and O_{ot} next to OH_{br}. Increasing the overpotential the OH_{br} structure releases protons so that for $\eta>0.19$ V and pH = 0 the thermodynamically most stable surface shifts from $(1\,OH_{br}1O_{br}+2\,O_{ot})$ to $(2\,O_{br}+2\,O_{ot})$ (Figure 1).

For the CER over RuO_2, essentially three reaction mechanisms have been discussed, namely Volmer–Tafel, Volmer–Heyrovsky, and the Krishtalik mechanism.[3] Using the $(1O_{br}1OH_{br}+2O_{ot})$ surface, which we found to be most stable in the reaction environment, we examined the kinetics of these three possible reaction mechanisms by DFT calculations employing harmonic transition theory and microkinetic modeling. The corresponding energy profiles for the three suggested mechanisms are presented in the Supporting Information, Section 3. According to these energy profiles, the Volmer–Heyrovsky mechanism is clearly favored.

The Volmer–Heyrovsky mechanism[19,20] consists of the adsorption and discharge of a chloride anion (Volmer step) on the O_{ot} site, which is followed by the direct recombination of the adsorbed chlorine species O_{ot}–Cl with a chloride anion from the electrolyte solution and the release of Cl_2 (Heyrovsky step):

$$(\mathrm{i})\rightarrow(\mathrm{ii}):\ \ O_{ot}+2\,Cl^-\rightarrow O_{ot}\text{–}Cl+e^-+Cl^- \qquad \text{(Volmer step)}$$

$$(\mathrm{ii})\rightarrow(\mathrm{iii}):\ \ O_{ot}\text{–}Cl+Cl^-\rightarrow O_{ot}+Cl_2+e^- \qquad \text{(Heyrovsky step)}$$

In the following, we comprehend on the thermodynamics and the kinetics of the CER over $RuO_2(110)$ based on the Volmer–Heyrovsky mechanism.

For the active surface in reactive environment, namely $(1\,O_{br}1\,OH_{br}+2\,O_{ot}$; Figure 1), the free-energy barriers for Volmer step (i) and Heyrovsky step (ii) are calculated for the two different active site configurations, O_{ot} next to O_{br} and O_{ot} next to OH_{br} at an electrode potential of $U=1.36$ V vs. SHE and pH = 0. The results are summarized in Figure 2. The thermodynamics of the Volmer and Heyrovsky step for the two different surface terminations is quantified with the Gibbs energy loss ΔG_{loss}, which describes the elementary reaction step that is most uphill in free energy under reaction conditions ($U=1.36$ V vs. SHE and pH = 0).

It turns out that the Volmer step (i) defines the Gibbs energy losses (thermodynamics) with values of $\Delta G_{loss}{}^{Vol}=0.34$ eV and $\Delta G_{loss}{}^{Vol}=0.25$ eV for the formation of the reaction intermediate OCl_{ot} next to O_{br} and OCl_{ot} next to OH_{br}, respectively. However, only for the active O_{ot} next to an O_{br} site, the Volmer step (i)→(ii) constitutes also the elementary reaction step with highest free energy barrier (kinetics) quantified with $\Delta G^{\#\,Vol}=0.68$ eV. Quite in contrast, for the active O_{ot} next to OH_{br} configuration the Heyrovsky step (ii)→(iii) displays the elementary reaction step with highest free energy barrier of $\Delta G^{\#\,Hey}=0.72$ eV. Therefore, both the Volmer and the Heyrovsky step may constitute rate-determining reaction steps for the CER over $RuO_2(110)$ depending on the considered active site of the catalyst.

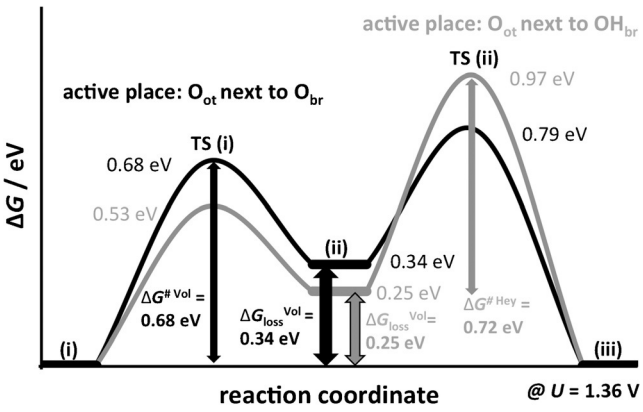

Figure 2. Gibbs energy diagrams for the CER over the $RuO_2(110)$-$(1\,OH_{br}1\,O_{br}+2\,O_{ot})$ surface according to the Volmer–Heyrovsky mechanism for an applied electrode potential of $U=1.36$ V vs. SHE and pH = 0. Transition states are denoted with abbreviation TS. Thick horizontal lines indicate the reaction intermediates. Black: active site O_{ot} next to O_{br}; gray: active site O_{ot} next to OH_{br}.

The energy profile in Figure 2 reveals that in case of the active O_{ot} next to OH_{br} site the thermodynamically limiting reaction step is not associated with the rate-determining reaction step (rds). Previously, Koper[21] has discussed this relation of ab initio thermodynamics with kinetics from a quite general viewpoint exemplified with the hydrogen evolution reaction (HER), emphasizing that thermodynamics may in some cases be a good descriptor for the kinetics of an electrocatalyzed reaction but in other cases may fail. This ambivalent situation is encountered with the CER over $RuO_2(110)$.

The first-principles kinetic analysis for the CER over $RuO_2(110)$ reveals that both the Volmer and the Heyrovsky step can be rate-determining for CER over $RuO_2(110)$, whereas the thermodynamic analysis indicates the Volmer step to be thermodynamically limiting for both active configurations. The thermodynamic analysis predicts that the O_{ot} next to an OH_{br} site should be more active than the O_{ot} next to an O_{br} site due to the smaller Gibbs energy loss. However, this conclusion conflicts with the present first-principles kinetic analysis in that the reverse relation is observed owing to the smaller free energy barrier. The observed discrepancy may be a more general problem: Within the BEP relation[22] the activation barriers are linearly related to the corresponding reaction energies. Therefore, a lowering of the Gibbs energy loss will reduce the barrier of endergonic reaction step (Volmer step), but concomitantly will increase the barrier for

the subsequent exergonic step (Heyrovsky step). This behavior is observed in Figure 2.

The thermodynamic approach works out under the tacit assumption that the actual activation barrier is dominated by thermodynamics (ΔG_{loss}) rather than by additional kinetic constraints. This assumption is not fulfilled for the CER over RuO_2(110) (Figure 2), and we surmise that it is neither fulfilled for some other electrochemical reactions such as the oxygen and hydrogen evolution reaction (OER/HER), nor the oxygen reduction reaction (ORR). In general, the overall activation barrier for an (electrochemical) reaction at room temperature is about 0.7 eV at an overpotential associated with a current densities of typically 10 mA cm^{-2}, while calculated Gibbs energy losses are reported to be only in the range of 0.2–0.4 eV.[23–28] For the electrochemical CO reduction over Cu(111), Nie et al.[29] found that the predicted product branching changed dramatically when besides the free energy analysis[30] also the kinetics of the elementary steps was considered. For the electroreduction of CO to C_2 species on Cu(100) electrodes the thermodynamics approach works, however, reliably as the additional activation barrier due to kinetics amounts only to 0.42 eV, while the Gibbs energy loss is 0.6 eV.[31] The thermodynamics approach is useful whenever the energy penalties are very high for specific adsorption sites, thus helping to identify the catalytically active sulfur species of amorphous MoS_x in the HER.[32]

A fundamental quantity in the field of electrode kinetics constitutes the so-called Tafel slope, which quantifies by how much the applied electrode potential has to be raised to increase the current density by one order of magnitude.[33–35] In case of the CER over RuO_2(110), the experimental Tafel slope turns out to be 40 mV dec^{-1} for small overpotentials, whereas the Tafel slope significantly rises up to a value of about 80 mV dec^{-1} for higher overpotentials.[5,6]

Based on our full kinetics study from first principles, the Tafel slope for the CER over RuO_2(110) is calculated by microkinetic modeling within the Volmer–Heyrovsky mechanism and compared to corresponding experiments. For the Volmer step and Heyrovsky step the reverse reactions, that is, the desorption of adsorbed chlorine into the electrolyte solution and the reduction of gaseous chlorine to chloride, respectively, are allowed to proceed. Therefore, the following reaction equations with rate constants k_1 for the Volmer step, k_{-1} for the reverse Volmer step, k_2 for the Heyrovsky step and k_{-2} for the reverse Heyrovsky step enter the microkinetic model:

$$O_{ot} + Cl^- \xrightarrow{k_1} OCl_{ot} + e^- \quad (1)$$

$$OCl_{ot} + e^- \xrightarrow{k_{-1}} O_{ot} + Cl^- \quad (2)$$

$$OCl_{ot} + Cl^- \xrightarrow{k_2} O_{ot} + Cl_2 + e^- \quad (3)$$

$$O_{ot} + Cl_2 + e^- \xrightarrow{k_{-2}} OCl_{ot} + Cl^- \quad (4)$$

The reaction rate r for the formation of the product chlorine, which is proportional to the current density j, is then given by the following equation:

$$j \sim r = \frac{dp(Cl_2)}{dt} = k_2(\eta)\cdot\theta_{Cl}(\eta)\cdot a(Cl^-) - k_{-2}(\eta)\cdot\theta_O(\eta)\cdot a(e^-)\cdot a(Cl_2) \quad (5)$$

A complete derivation of the mathematical model for the construction of the Tafel plot is presented in the Supporting Information, Sections 4,5. The activity of chloride, electrons, and chlorine are assumed to be constant, $a(Cl^-) = a(e^-) = a(Cl_2) = 1$. The coverages of chlorine θ_{Cl} and of oxygen θ_O on the catalyst's surface are calculated assuming steady-state conditions. The rate constants k_2 and k_{-2} are determined applying transition state theory and are affected by the applied overpotential η via the symmetry factor α. We need to emphasize that all parameters in Equation (5) are determined from first principles, except for the symmetry factor α that was chosen to be 0.5. In the supporting information we indicate that the derived microkinetics is practically independent of the chosen value of α when varied in the range of 0.25 to 0.75. In Figure 3 the applied overpotential η as a function of the logarithm of the current density log(j) is depicted which establishes the so-called Tafel plot. The theoretical Tafel plot (cf. Figure 3) reveals two regions. For $\eta < 0.1$ V a Tafel slope of 42 mV dec^{-1} is found, in good agreement with experimental data.[5,6] Increasing the overpotential leads to a significant rise in the value of the Tafel slope quantified with 85 mV dec^{-1} in the second Tafel region ($\eta > 0.15$ V). This finding agrees well with experimental data of Guerrini et al.[6] (Figure 3), determining a Tafel slope of 40 mV dec^{-1} for $\eta < 0.07$ V and 88 mV dec^{-1} for $\eta > 0.12$ V.

A switch of the Tafel slope is frequently discussed in terms of a change in the rate-determining reaction step (rds) or even the reaction mechanism. This is obviously not the case here, where the Tafel slope changes substantially without changing the reaction mechanism or the rds. A similar effect was previously observed in the electro oxidation of CO on Pt.[36]

The generalized Butler–Volmer equation[37–39] reveals that the current density j depends on the rate-determining reaction step and on the exchange current density j_0, which is a function of the surface coverage θ_{Cl} of chlorine on the catalyst's surface. Our kinetic study from first-principles clearly demonstrates that the surface chlorine coverage θ_{Cl} is a strong function of the applied overpotential η (inset in

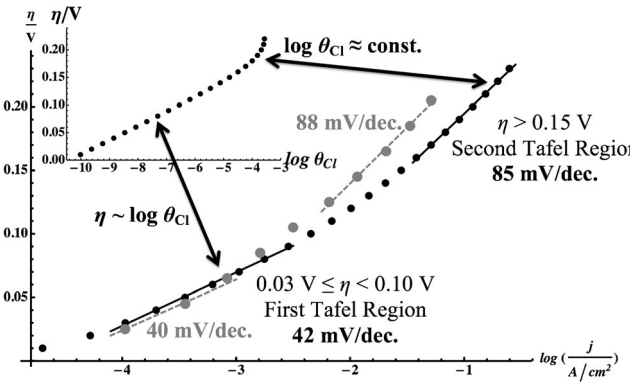

Figure 3. Theoretically calculated Tafel plot (black dots) for the CER over RuO_2(110) agrees remarkably well with the experimental Tafel plot (gray dots).[6] The current densities are multiplied by a scaling factor of 100 to match the theoretical data (see the Supporting Information, Section 5 for a detailed discussion). In the first Tafel region the surface coverage of chlorine θ_{Cl} is strongly affected by the applied overpotential (inset), whereas in the second Tafel region the chlorine coverage is approximately constant.

Figure 3). It turns out that in the first Tafel region the surface coverage of chlorine rises significantly by several orders of magnitude, whereas for higher overpotentials the chlorine surface coverage varies much less dramatically with the overpotential. Consequently, the change in the Tafel slope from 42 mV dec^{-1}. to 85 mV dec^{-1} is mainly ascribed to the variation of chlorine surface coverage, while the rate-determining reaction step remains unchanged.

In conclusion, a full kinetic study from first principles allows us to gain unprecedented molecular insight into the CER over RuO_2(110), starting from the stable reaction intermediates (ab initio thermodynamics), computing the energy barriers (kinetics) and finally performing microkinetic modeling, all investigated in the presence of the electrochemical environment and parameters. We showed that the Volmer–Heyrovsky mechanism is the most favorable mechanistic description of the CER over RuO_2(110). The theoretically determined Tafel slope (based on microkinetic modeling from first principles) agrees well with the corresponding experimental data. We demonstrate that the experimentally observed change in the Tafel slope is not related to an alteration of the rate-determining reaction step or the reaction mechanism, but rather is ascribed to the potential dependent variation of chlorine surface coverage. We are confident that full kinetic studies from first-principles are not only required for the CER over RuO_2(110) model system, but may be beneficial whenever detailed molecular insight into an electrocatalytic reaction is pursued.

Acknowledgements

K.S.E. acknowledges financial support by the Fonds Chemischer Industrie (FCI) via a PhD scholarship. T.J. acknowledges support from the DFG (Deutsche Forschungsgemeinschaft) and the European Research Council through the ERC-Starting Grant THEOFUN (Grant Agreement No. 259608).

Keywords: chlorine evolution · density functional calculations · electrocatalysis · reaction kinetics · ruthenium dioxide

How to cite: *Angew. Chem. Int. Ed.* **2016**, *55*, 7501–7504
Angew. Chem. **2016**, *128*, 7627–7630

[1] EuroChlor, *Chlorine Industry Review* **2013 – 2014**.
[2] S. Trasatti, *Electrochim. Acta* **2000**, *45*, 2377.
[3] S. Trasatti, *Electrochim. Acta* **1987**, *32*, 369.
[4] H. Over, *Chem. Rev.* **2012**, *112*, 3356.
[5] V. Consonni, S. Trasatti, F. Pollak, W. E. O'Grady, *J. Electroanal. Chem.* **1987**, *228*, 393.
[6] E. Guerrini, V. Consonni, S. Trasatti, *J. Solid State Electrochem.* **2005**, *9*, 320.
[7] H. A. Hansen, I. C. Man, F. Studt, F. Abild-Pedersen, T. Bligaard, J. Rossmeisl, *Phys. Chem. Chem. Phys.* **2010**, *12*, 283.
[8] J. Rossmeisl, Z.-W. Qu, H. Zhu, G.-J. Kroes, J. K. Norskov, *J. Electroanal. Chem.* **2007**, *607*, 83.
[9] J. K. Nørskov, J. Rossmeisl, A. Logadottir, L. Lundquist, J. R. Kitchin, T. Bligaard, H. Jonsson, *J. Phys. Chem. B* **2004**, *108*, 17886.
[10] J. K. Nørskov, T. Bligaard, A. Logadottir, J. R. Kitchin, J. G. Chen, S. Pandelov, U. Stimming, *J. Electrochem. Soc.* **2005**, *152*, J23.
[11] C. D. Taylor, S. A. Wasileski, J. S. Fishol, M. Neurock, *Phys. Rev. B* **2006**, *73*, 165402.
[12] A. B. Anderson, *Electrocatalysis* **2012**, *3*, 176.
[13] M. T. M. Koper, *Chem. Sci.* **2013**, *4*, 2710.
[14] T. Jacob in *Fuel Cell Catalysis: A Surf. Sci. Approach* (Eds.: M. T. M. Koper, A. Wieckowski), Wiley, Hoboken, **2009**, p. 129.
[15] K. S. Exner, J. Anton, T. Jacob, H. Over, *Electrochim. Acta* **2014**, *120*, 460.
[16] a) K. S. Exner, J. Anton, T. Jacob, H. Over, *Angew. Chem. Int. Ed.* **2014**, *53*, 11032; *Angew. Chem.* **2014**, *126*, 11212; b) K. S. Exner, J. Anton, T. Jacob, H. Over, *Angew. Chem.* **2014**, *126*, 11212.
[17] S. Siahrostami, A. Vojvodic, *J. Phys. Chem. C* **2015**, *119*, 1032.
[18] L. D. Burke, J. F. O'Neill, *J. Electroanal. Chem.* **1979**, *101*, 341.
[19] S. Trasatti, G. Lodi, in *Electrodes of Conductive Metallic Oxides Anodes, Part B* (Ed.: S. Trasatti), Elsevier, Amsterdam, **1981**, p. 521.
[20] L. J. J. Janssen, L. M. C. Starman, J. G. Visser, E. Barendrecht, *Electrochim. Acta* **1977**, *22*, 1093.
[21] M. T. M. Koper, *J. Solid State Electrochem.* **2013**, *17*, 339.
[22] a) J. N. Bronsted, *Chem. Rev.* **1928**, *5*, 231; b) M. G. Evans, M. Polanyi, *Trans. Faraday Soc.* **1938**, *34*, 11.
[23] a) V. Stamenkovic, B. S. Mun, K. J. J. Mayrhofer, P. N. Ross, N. M. Markovic, J. Rossmeisl, J. Greeley, J. K. Norskov, *Angew. Chem. Int. Ed.* **2006**, *45*, 2897; *Angew. Chem.* **2006**, *118*, 2963; b) V. Stamenkovic, B. S. Mun, K. J. J. Mayrhofer, P. N. Ross, N. M. Markovic, J. Rossmeisl, J. Greeley, J. K. Norskov, *Angew. Chem.* **2006**, *118*, 2963.
[24] D. Friebel, M. W. Louie, M. Bajdich, K. E. Sanwald, Y. Cai, A. M. Wise, M.-J. Cheng, D. Sokaras, T.-C. Weng, R. Alonso-Mori, R. C. Davis, J. R. Bargar, J. K. Norskov, A. Nilsson, A. T. Bell, *J. Am. Chem. Soc.* **2015**, *137*, 1305.
[25] M. Bajdich, M. Garcia-Mota, A. Vojvodic, J. K. Norskov, A. T. Bell, *J. Am. Chem. Soc.* **2013**, *135*, 13521.
[26] G. Greeley, T. F. Jaramillo, J. Bonde, I. Chorkendorff, J. K. Norskov, *Nat. Mater.* **2006**, *5*, 909.
[27] S. Siahrostami, A. Verdaguer-Casadevall, M. Karamad, D. Deiana, P. Malacrida, B. Wickman, M. Escudero-Escribano, E. A. Paoli, R. Frydendal, T. W. Hansen, I. Chorkendorff, I. E. L. Stephens, J. Rossmeisl, *Nat. Mater.* **2013**, *12*, 1137.
[28] I. E. L. Stephens, A. S. Bondarenko, U. Gronbjerg, J. Rossmeisl, I. Chorkendorff, *Energy Environ. Sci.* **2012**, *5*, 6744.
[29] X. Nie, M. R. Esopi, M. H. Janik, A. Asthagiri, *Angew. Chem. Int. Ed.* **2013**, *52*, 2459; *Angew. Chem.* **2013**, *125*, 2519.
[30] A. A. Peterson, F. Abild-Pederson, F. Studt, J. Rossmeisl, J. K. Norskov, *Energy Environ. Sci.* **2010**, *3*, 1311.
[31] F. Calle-Vallejo, M. T. M. Koper, *Angew. Chem. Int. Ed.* **2013**, *52*, 7282; *Angew. Chem.* **2013**, *125*, 7423.
[32] L. R. L. Ting, Y. Deng, L. Ma, Y.-J. Zhang, A. A. Peterson, B. S. Yeo, *ACS Catal.* **2016**, *6*, 861.
[33] E. Gileadi, *J. State State Electrochem* **2011**, *15*, 1359.
[34] B. V. Tilak, E. Conway, *Electrochim. Acta* **1992**, *37*, 51.
[35] G. Inzelt, *J. Solid State Electrochem.* **2011**, *15*, 1373.
[36] M. T. M. Koper, A. P. Jansen, R. A. van Santen, J. J. Lukkine, P. A. J. Hibers, *J. Chem. Phys.* **1998**, *109*, 6051.
[37] R. Parsons, *Trans. Faraday Soc.* **1958**, *54*, 1053.
[38] J.O'M. Bockris, A. K. N. Reddy, *Modern Electrochemistry 2*, Plenum/Rosetta, New York, **1970**.
[39] S. Fletcher, *J. Solid State Electrochem.* **2009**, *13*, 537.

Received: December 21, 2016
Revised: March 23, 2016
Published online: May 11, 2016

